Technical Report

Department of Computer Science
and Engineering
University of Minnesota
4-192 EECS Building
200 Union Street SE
Minneapolis, MN 55455-0159 USA

TR 11-003

Energy Optimal Velocity Profiles for Car-like Robots

Pratap Tokekar, Nikhil Karnad, and Volkan Isler

February 09, 2011

Energy Optimal Velocity Profiles for Car-Like Robots

Pratap Tokekar, Nikhil Karnad and Volkan Isler

***Abstract*—For battery-powered mobile robots to operate for long periods of time, it is critical to optimize their motion so as to minimize energy consumption. The driving motors are a major source of power consumption. In this paper, we study the problem of finding energy-efficient velocity profiles for car-like robots given a path to travel.**

We start with an established model for energy consumption of DC motors. First, we study the problem of computing an optimal velocity profile for a car-like robot so as to minimize the energy consumed while traveling along a given path. We present closed form solutions for the unconstrained case and for the case where there is a bound on maximum velocity. We also study a general problem where the robot's path is composed of segments (e.g. circular arcs and line segments). We are given a velocity bound for each segment. For this problem, we present a dynamic programming solution which uses the solution for the single-constraint case as a subroutine. In addition, we present a calibration method to find model parameters. Finally, we present results from experiments conducted on a custom-built robot.

I. Introduction

In this work, we study the problem of energy efficient navigation. Specifically, we focus on car-like robots powered by DC motors. It is well-known that the energy consumption of a DC motor depends on the angular velocity and acceleration. We study the problem of computing the velocity profile of a robot so that it consumes a minimum amount of energy to travel along a given path.

Even though energy efficient navigation is a fundamental problem, it has received very little attention, and a comprehensive treatment is missing. Existing literature includes the work of Sun and Reif [12] who consider the problem of computing the optimal path over a terrain. Under the assumption that the friction coefficients are known across the terrain, they show how to compute a path that requires minimum energy to overcome frictional forces. This work generates the path but does not yield an optimal velocity and acceleration profile. In this sense, it is complementary to the present work.

In order to compute the velocity and acceleration profiles, power consumption needs to be modeled. Mei et al. [10] model the power consumption as a sixth-degree polynomial of the robot's speed using experimentally collected data. However, their model does not incorporate acceleration. More importantly, they use this model to compare velocity profiles but do not address the problem of computing an optimal profile.

P. Tokekar, N. Karnad and V. Isler are with the Department of Computer Science and Engineering, University of Minnesota, 200 Union Street SE, Minneapolis MN 55414 USA. e-mail: {tokekar, karnad, isler}@cs.umn.edu.

P. Tokekar is the corresponding author.

Kim and Kim [8] find the optimal velocity profile for a robot moving on a straight line, when the total time to travel is fixed. However, this solution does not incorporate any bound on maximum velocity of the robot. In [7], they propose a minimum energy rotational trajectory that minimizes the energy. They do not present a systematic method to combine the solutions for translational and rotational trajectories. Thus, it is not clear if this approach yields an optimal solution. Wang et al. [13] studied the problem of finding a minimum energy trapezoidal velocity profile. As we will show shortly, trapezoidal profile itself is not optimal in terms of total energy consumption. In addition, they too do not consider any upper bound on the velocity of the robot. Further, their technique is only applicable for turn-in-place-move-forward type of motion for differential drives, and is not experimentally verified.

The general problem we study can be considered a type of kinodynamic planning problem. In the standard version of kinodynamic planning, the objective is to minimize the travel time while satisfying velocity and acceleration constraints [4]. Here, we focus on energy instead. The pioneering work for finding shortest paths for a forward-only car-like robot was done by Dubins [5]. Reed and Shepps [11] extended this work for a car that can go forward and backward. Balkcom and Mason [2] used optimal control techniques to give the time optimal trajectories for bounded velocity differential drives. Recently, Chitsaz et al. [3] used similar techniques to give the complete characterization for minimum wheel rotation paths for differential drive robots. In this work, we do not address the problem of computing an energy efficient path. Instead, we assume that the path is given. Even when the path is given, minimizing energy is a non-trivial optimal control problem.

The rest of the paper is organized as follows: After presenting the formal problem-statement and the energy model in Section II, we present a calibration procedure for estimating the parameters of the energy model in Section III. The optimal velocity profiles with and without a maximum velocity bound are derived in Section IV and Section V respectively. The application of these results to compute the velocity profile over an entire path composed of multiple segments is presented in Section VI. Experiments on our custom-robot are presented in Section VII. We conclude with a discussion on the utility of our results in Section VIII.

II. Problem Formulation

We are given a path $\mathbf{\Pi}$ along which the robot moves. Let D be its total length. Since the motion of the robot is restricted to $\mathbf{\Pi}$, we can represent the instantaenous position by a single

parameter,$x(t)$. The forward velocity and acceleration of the robot are represented by $v(t)$ and $a(t)$ respectively. We define the state of the robot by $\mathbf{X}(t) = [x(t),\ v(t)]^T$. The state transition equation can be written as,

$$\dot{\mathbf{X}}(t) = \begin{bmatrix} \dot{x}(t) \\ \dot{v}(t) \end{bmatrix} = \begin{bmatrix} v(t) \\ a(t) \end{bmatrix} \tag{1}$$

The problem we address in this paper is to compute the velocity profile, $v(t)$, of the robot along $\mathbf{\Pi}$ which minimizes the energy consumption for motion. In this section, we present the energy model that we use and then formally state the problem that we solve.

A. Energy Model

We use the model described in [1] for energy consumption in a brushed DC motor. This detailed model considers the energy dissipated in the resistive winding, the energy required to overcome internal and load friction and the mechanical power delivered to the output shaft. The instantaneous current $i(t)$ in the motors is given by,

$$i(t) = \frac{1}{K_T}\Big[T_F + T_L + D_f\omega(t) + (J_M + J_L)\frac{d\omega(t)}{dt}\Big] \tag{2}$$

and the voltage $e(t)$ across the motor is given by,

$$e(t) = i(t)R + K_E\omega(t) \tag{3}$$

where $\omega(t)$ is the angular velocity of the motor, K_E and K_T are back-EMF and torque constants, T_F and T_L are internal and load frictional torques, D_f is the internal damping force and J_M and J_L are motor and load moments of inertia.

Parameters such as T_L and J_L depend on the characteristics of the wheel and the nature of the surface on which the robot is moving. The internal parameters of the motors commonly used in robots are rarely given. However, to use the energy model, we do not need to know the individual motor parameters. For a given flat surface, instantaneous power and energy consumption depend only on the velocity and acceleration while all the other parameters remain constant.

We can rewrite Equations 2 and 3 in terms of the motor angular velocity and acceleration by substituting:

$$\begin{aligned} i(t) &= a_1 + a_2\omega(t) + a_3\frac{d\omega(t)}{dt}, \\ e(t) &= a_4 + a_5\omega(t) + a_6\frac{d\omega(t)}{dt}. \end{aligned} \tag{4}$$

where $a_1, \ldots, a_6$ are constants obtained as combinations of various motor parameters. Let r be the radius of the wheel and N_g be the gear ratio of the shaft. We can rewrite (4) in terms of the linear velocity of the wheel $v(t)$ and acceleration $a(t)$ by substituting $\omega(t) = v(t)/(N_g r)$ and using new constants $b_1, \ldots, b_6$.

$$\begin{aligned} i(t) &= b_1 + b_2 v(t) + b_3 a(t), \\ e(t) &= b_4 + b_5 v(t) + b_6 a(t). \end{aligned} \tag{5}$$

The equation for energy consumption is given by,

$$\begin{aligned} E &= \int_0^{t_f} \Big[e(t)i(t)\Big]dt, \\ &= \int_0^{t_f} \Big[c_1 a^2(t) + c_2 v^2(t) + c_3 v(t) \\ &\quad + c_4 + c_5 a(t) + c_6 v(t)a(t)\Big]dt. \end{aligned}$$

where constants $c_1, \ldots, c_6$ are combinations of $b_1, \ldots, b_6$.

We assume that over the path $\mathbf{\Pi}$, the robot starts from and returns to rest. When the initial and final velocity values are the same, the net contribution by the terms corresponding to c_5 and c_6 is zero. Hence, we can rewrite the above Equation as,

$$E = \int_0^{t_f} \Big[c_1 a^2(t) + c_2 v^2(t) + c_3 v(t) + c_4\Big]dt. \tag{6}$$

The constants $c_1, \ldots, c_4$ depend on the motor parameters which in turn depend on the robot design and the surface on which the robot is moving. These parameters can be obtained using the calibration procedure presented in Section III.

B. Problem Statement

Recall that $\mathbf{\Pi}$ is a path of length D. The energy consumption for a velocity profile $v(t)$ traversing $\mathbf{\Pi}$ is given by Equation 6.

The final time t_f can be fixed or kept a free variable. We study three problems of increasing generality. For each of the problems, the objective is to minimize E subject to the constraints given below:

Problem 1: There is no bound on the maximum velocity of the robot. The robot starts from and returns to rest i.e., the initial boundary conditions are given as,

$$x(0) = 0, \quad v(0) = 0, \tag{7}$$

and the final boundary conditions are given as,

$$x(t_f) = D, \quad v(t_f) = 0. \tag{8}$$

Problem 2: The maximum velocity of the robot over $\mathbf{\Pi}$ is bounded by v_m, i.e.,

$$v(t) \leq v_m, \quad 0 \leq t \leq t_f. \tag{9}$$

The initial and final velocities of the robot can be non-zero, i.e., $v(0) = v_0$ and $v(t_f) = v_f$ subject to $v_0, v_f \leq v_m$.

Problem 3: $\mathbf{\Pi}$ consists of N segments made up of straight lines and curves. There is a separate velocity bound for each segment. For each segment i, we are given the velocity bound $v_m(i)$ and the distance to travel $D(i)$, $1 \leq i \leq N$. The objective is to find the optimal velocity profile over the entire path $\mathbf{\Pi}$. The robot starts from rest and returns to rest at the end of the path.

The solutions for *Problems 1, 2* and *3* are presented in Sections IV, V and VI respectively. While deriving the model, we assumed that the initial and final velocity is the same. However, for *Problem 2* we consider non-zero terminal conditions. This case is used only as a subroutine for *Problem 3*, where the initial and final velocity is zero for the first and last segment, respectively. The resulting solution over all the segments remains optimal.

III. Calibration

In this section, we describe a simple procedure to find the energy model (Equation 6) of the robot for a given flat surface. We use a custom-built robot (see Figure 1(a)) for experiments. The robot is driven using two DC motors whose output shafts are connected together. It has car-like steering controlled by an independent servo motor. Separate batteries are used to drive the DC motors and power the rest of the electronics on the robot.

(a) Custom-built robot used in our experiments.

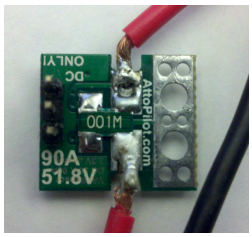

(b) Attopilot voltage and current measurement circuit from SparkFun Electronics.

Fig. 1. Experimental setup.

A. Experimental Setup

Our method utilizes a simple current and voltage measurement circuit (Figure 1(b)) connected between the output of the motor driver circuit and the motor. This circuit measures the current flowing and voltage across the motor. A low-level micro-controller on the robot is interfaced with this circuit to log the current and voltage values in its memory. The micro-controller is programmed to drive the robot at any set velocity. An optical encoder is installed on one of the wheels. The micro-controller takes feedback from the encoders to measure the actual velocity and adjusts the Pulse Width Modulation (PWM) signal for the motor driver to correct for the error with respect to set velocity. In the calibration procedure described next, the steering of the robot is set to make the robot move in a straight line.

B. Calibration Procedure

The calibration procedure to obtain the energy parameters consists of the following steps:

STEP 1: The robot must be programmed to accelerate from rest and reach a particular set velocity v_{set}, on the surface for which the energy parameters are to be computed. The robot must then move at v_{set} for some predefined time interval. Repeat for different v_{set} values ranging from 0 to v_m, where v_m is the maximum achievable velocity for the robot. Figure 2 (a) shows some of the actual profiles obtained during calibration for v_{set} from $0.5m/s$ to $2.5m/s$. Current and voltage across the motor must be logged throughout this run.

STEP 2: For each trial, compute the average current and voltage values for the period where the robot was moving at v_{set}, neglecting the initial portion where the robot is accelerating. Plot these average current and voltage values with respect to v_{set}. Figure 2 (b and c) show the plots for current values obtained during the calibration.

STEP 3: From Equation 5, we know that current and voltage bear a linear relationship with v_{set}, when the robot is not accelerating i.e., $a(t) = 0$. Hence, we can find the parameters b_1, b_2, b_4 and b_5 using least-squares linear fitting to the data obtained in the previous step (see Figure 2 (b and c)). Here, the terms b_1 and b_4 represent the current that flows and voltage that must be applied for the robot to overcome inertia.

STEP 4: To find the remaining two terms b_3 and b_6 in the model, we program the robot move from rest at a particular set acceleration value a_{set}. Similar to earlier steps, we repeat this trial for various a_{set} values. Figure 2(d) shows four such trials with varying a_{set} values.

STEP 5: For each trial, for every data point collected, we can compute the value of b_3 and b_6 as,

$$b_3 = \frac{1}{a_{set}} \left[i(t) - b_1 - b_2 v(t) \right],$$
$$b_6 = \frac{1}{a_{set}} \left[v(t) - b_4 - b_5 v(t) \right].$$

In the above equations, all values except b_3 and b_6 are known. The final values of b_3 and b_6 used in the model can be found by averaging these obtained for each data point.

STEP 6: Finally, the required parameters $c_1, \ldots, c_4$ in the model used throughout the paper (Equation 6) can then be calculated as $c_1 = b_3 b_6$, $c_2 = b_2 b_5$, $c_3 = b_1 b_5 + b_2 b_4$, and $c_4 = b_1 b_4$.

Using the above procedure, we calibrated our robot on two surfaces: smooth corridor indoors and grass outdoors. The parameters obtained for each are listed in Table I.

Surface	c_1	c_2	c_3	c_4
Corridor	17.75	1.16	10.46	4.70
Grass	7.68	4.39	24.67	14.77

TABLE I
ENERGY MODEL PARAMETERS (*SI units*) OBTAINED USING THE CALIBRATION PROCEDURE.

The rest of the paper uses the parameters obtained for the corridor surface for illustrations.

IV. Optimal unconstrained velocity profile

In this section, we present the solution to *Problem 1*. We first state the necessary conditions and present the closed form solution for the optimal velocity profile. Then, we discuss and provide insights for the structure of the optimal profile. Finally, we compare the optimal profile with the commonly-used trapezoidal velocity profile.

A. Solution

When there is no bound on the maximum velocity, the Hamiltonian for this problem can be obtained using Equations 1 and 6 as,

$$\begin{aligned} H(\mathbf{X}(t), a(t), \boldsymbol{\lambda}(t), t) \quad &= c_1 a^2(t) + c_2 v^2(t) + c_3 v(t) \\ &+ c_4 + \lambda_1(t) v(t) + \lambda_2(t) a(t) \end{aligned} \quad (10)$$

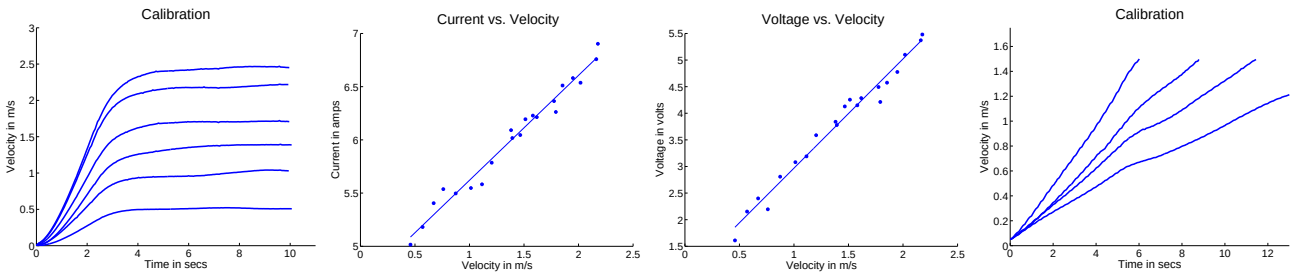

Fig. 2. Figures obtained during calibration on the corridor surface. Left to right: **(a)** The robot initially accelerates from rest to various set velocity values. Feedback from the encoders is used to maintain v_{set}. The average current and voltage is computed for the region where the robot has reached v_{set} (STEP 1). **(b)** Current consumption as a function of the velocity, when the motor is not accelerating. Least-squares linear fitting was used to determine the parameters b_1 and b_2 in Equation 5 (STEPS 2 and 3). **(c)** Voltage applied to the motor as a function of the velocity, when the motor is not accelerating. Least-squares linear fitting was used to determine the parameters b_4 and b_5 in Equation 5 (STEPS 2 and 3). **(d)** Calibration procedure to determine the parameters b_3 and b_6 from Equation 5. The robot is accelerated with various set acceleration values a_{set} while logging current and voltage values (STEP 4).

where $\lambda_1(t)$ and $\lambda_2(t)$ are the Lagrange multipliers, also called the co-state variables and the acceleration $a(t)$ is the control.

The three necessary conditions for $a^*(t)$ to optimize the Hamiltonian [9] for all time $t \in [0, t_f]$ are given as,

$$\dot{\mathbf{X}}^*(t) = \frac{\partial H}{\partial \boldsymbol{\lambda}}, \quad \dot{\boldsymbol{\lambda}}^*(t) = -\frac{\partial H}{\partial \mathbf{X}}, \quad 0 = \frac{\partial H}{\partial a} \tag{11}$$

Applying these necessary conditions, we can solve for the optimal control and states to get,

$$a^*(t) = ks_1e^{kt} - ks_2e^{-kt} \tag{12}$$

$$v^*(t) = s_1e^{kt} + s_2e^{-kt} - \left(\frac{c_3 + s_3}{2c_1}\right) \tag{13}$$

$$x^*(t) = \frac{s_1e^{kt}}{k} - \frac{s_2e^{-kt}}{k} - \left(\frac{c_3 + s_3}{2c_1}\right)t + s_4. \tag{14}$$

where $k = \sqrt{\frac{c_2}{c_1}}$ and $s_1 - s_4$ are constants.

We can solve for $s_1 - s_4$ in terms of the final time t_f by substituting the boundary conditions given in Equations 7 and 8 for $v^*(t)$ and $x^*(t)$. We obtain,

$$\begin{aligned} s_1 &= -\frac{Dk}{kt_f + e^{kt_f}(kt_f - 2) + 2}, \\ s_2 &= s_1e^{kt_f}, \\ s_3 &= 2c_1(s_1 + s_2) - c_3, \\ s_4 &= -\frac{s_1 - s_2}{k}. \end{aligned} \tag{15}$$

By substituting in Equations 12-14 we obtain,

$$\begin{aligned} a^*(t) &= D\left(\frac{c_2}{c_1}\right)\left(\frac{e^{k(t_f-t)} - e^{kt}}{kt_f + e^{kt_f}(kt_f - 2) + 2}\right), \\ v^*(t) &= D\sqrt{\frac{c_2}{c_1}}\left(\frac{(1 + e^{kt_f} - (e^{k(t_f-t)} + e^{kt}))}{kt_f + e^{kt_f}(kt_f - 2) + 2}\right), \\ x^*(t) &= D\left(\frac{(e^{k(t_f-t)} - e^{kt}) - (e^{kt_f} - 1) + kt(e^{kt_f} + 1)}{kt_f + e^{kt_f}(kt_f - 2) + 2}\right). \end{aligned} \tag{16}$$

Since the final time is free, it can be solved for using the additional boundary condition (known as the transversality condition) given by,

$$H(\mathbf{X}^*(t_f), a^*(t_f), \boldsymbol{\lambda}^*(t_f), t_f) = 0. \tag{17}$$

Substituting Equations 12-14 and 15 above results in,

$$(D\frac{c_2}{c_1} + 2)(1 - e^{kt_f}) + \sqrt{\frac{c_4}{c_1}}kt_f(1 + e^{kt_f}) = 0, \tag{18}$$

which is an equation in single variable t_f (all other terms are constant) and can be solved using any solvers. (We used MATLAB's `solve` function). Alternatively, if the final time is fixed, we can directly substitute this given value in Equation 16 to find $v^*(t)$.

B. Examples and observations

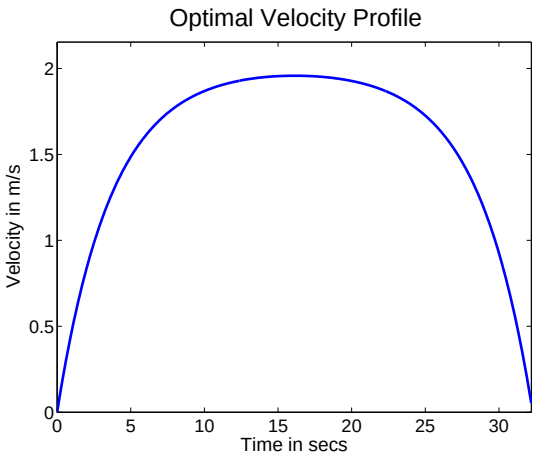

Fig. 3. The optimal velocity profile ($v^*(t)$) for distance $D = 50m$ using $c_1 - c_4$ obtained during calibration in Section III. The optimal profile is made up of symmetric exponential curves, reaching a maximum velocity at $t = t_f/2$.

Figure 3 shows the optimal velocity profile obtained for traveling a distance of 50m using Equation 16. It can be observed that the profile consists of symmetric acceleration and deceleration curves with an almost-constant velocity region in the middle. From Equation 16 and 18, we can show that the peak velocity is reached at $t = t_f/2$ and is given by, $v^*(\frac{t_f}{2}) = \sqrt{\frac{c_4}{c_2}}\frac{(e^{\frac{k}{2}t_f} - 1)}{(e^{\frac{k}{2}t_f} + 1)}$. The corresponding optimal control profile is shown in Figure 4. The acceleration profile is a smooth exponentially decreasing function. The acceleration is almost zero in the middle region (exactly zero at $t = t_f/2$).

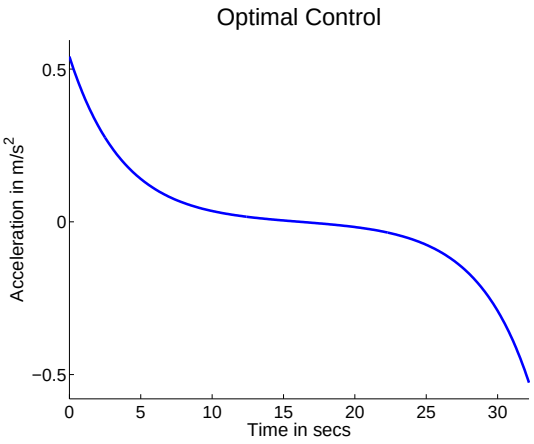

Fig. 4. Optimal Control ($a^*(t)$) obtained for traveling a distance of $D = 50m$ corresponding to the optimal velocity profile shown in Figure 3.

C. Structure of Optimal Profile

The optimal velocity profile shows similar structure when the distance to travel D is varied. Figure 5 shows the optimal velocity profiles for traveling various distances. The acceleration and deceleration curves are similar, with changes in the width of the near-constant velocity region depending on the distance. Note that these profiles are obtained without any bound on the maximum velocity of the robot.

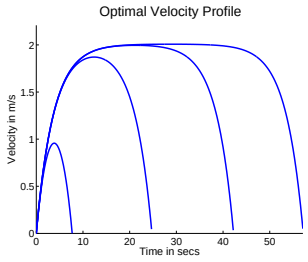

Fig. 5. Optimal Velocity ($v^*(t)$) profiles obtained for traveling different distances $D = 5, 35, 70, 100m$ follow a similar structure.

It is worth noting that the optimal profile reaches the same peak velocity and does not go faster even if the distance to travel increases. From the cost function (Equation 6), we see that both, higher velocities (through terms c_2 and c_3) and longer times (through c_4) are penalized by higher energy cost. Hence, this peak velocity value represents the energy trade-off between moving faster (and consequently for a lesser time) and moving slower (and for longer times). The following lemma sheds light on this underlying structure for the optimal velocity profiles.

Lemma 4.1: Consider an arbitrary velocity profile $v(t)$ traveling a distance D. Let the total energy consumption of $v(t)$ be E. If the given profile crosses $\sqrt{\frac{c_4}{c_2}}$ between times t_i and t_{i+1}, we can replace this section of $v(t)$, $t_i \leq t \leq t_{i+1}$ by a constant velocity section of $v_c = \sqrt{\frac{c_4}{c_2}}$, so that the resulting velocity profile covers the same distance and consumes energy less than $v(t)$.

Proof: Consider any velocity profile $v(t)$ shown in Figure 6. Let D and E be the total distance covered and energy consumed by $v(t)$. This profile crosses $\sqrt{\frac{c_4}{c_2}}$ between times $[t_1, t_2]$ and $[t_3, t_4]$. Let d_{12} and d_{34} be the distances covered by $v(t)$ in these sections. The total energy consumption of $v(t)$ is given by,

$$E = E_{01} + E_{12} + E_{23} + E_{34} + E_{45}, \tag{19}$$

where E_{ij} refers to the energy consumption to cover the distance d_{ij}.

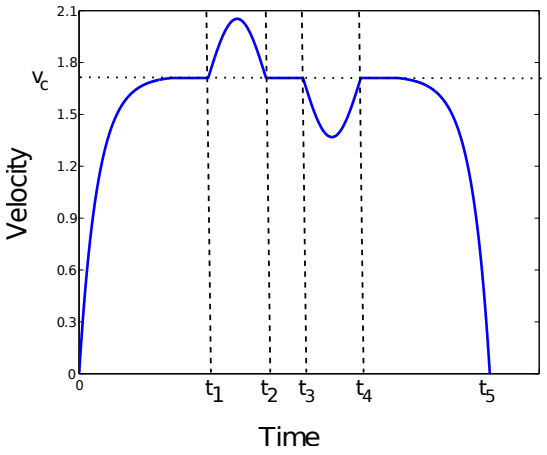

Fig. 6. Sections of this velocity profile crossing ($v_c = \sqrt{\frac{c_4}{c_2}}$) between $[t_1, t_2]$ and $[t_3, t_4]$ can be replaced by constant velocity (v_c) sections resulting in a velocity profile that consumes lesser energy to travel the same distance.

We construct another velocity profile $v'(t)$ by replacing the sections $[t_1, t_2]$ and $[t_3, t_4]$ by constant velocity $v_c = \sqrt{\frac{c_4}{c_2}}$ sections for time $\frac{d_{12}}{v_c}$ and $\frac{d_{34}}{v_c}$ respectively. The total distance traveled by $v'(t)$ is D, same as $v(t)$. The total energy consumption of $v'(t)$ is given by,

$$E' = E_{01} + E'_{12} + E_{23} + E'_{34} + E_{45}, \tag{20}$$

since $v'(t)$ is the same as $v(t)$ everywhere except $t \in [t_1, t_2]$ and $t \in [t_3, t_4]$. Note that $v'(t)$ is the same as $v(t)$ while covering the distances d_{01}, d_{23} and d_{45}. Consequently, the energy consumption differs only for d_{12} and d_{34}.

We now show that $E' \leq E$ by proving both $E'_{12} \leq E_{12}$ and $E'_{34} \leq E_{34}$. This result can then be generalized to velocity profiles with any number of crossing sections in either directions.

First, let us compute the energy consumption E_{12} for $v(t)$,

$$\begin{aligned} E_{12} &= \int_{t_1}^{t_2} \Big[c_1 a^2(t) + c_2 v^2(t) + c_3 v(t) + c_4\Big] dt, \\ &= \int_{t_1}^{t_2} \Big[c_1 a^2(t) + c_2 v^2(t) + c_4\Big] dt + c_3 \int_{t_1}^{t_2} v(t) dt, \\ &= \int_{t_1}^{t_2} \Big[c_1 a^2(t) + c_2 v^2(t) + c_4\Big] dt + c_3 d_{12}. \end{aligned} \tag{21}$$

Now, consider the energy consumed by $v'(t)$ to travel the same distance d_{12} at constant velocity v_c. The time taken in

this case would be $t_c = \frac{d_{12}}{v_c}$. The energy consumption is,

$$E'_{12} = \int_{t_1}^{t_c} \Big[c_1 a^2(t) + c_2 v^2(t) + c_3 v(t) + c_4\Big] dt,$$
$$= c_2 v_c d_{12} + c_3 d_{12} + c_4 \frac{d_{12}}{v_c}. \quad (22)$$

The distance d_{12} can also be written as,

$$d_{12} = \int_{t_1}^{t_2} [v(t)dt]\,. \quad (23)$$

Substituting Equation 23 in 22, we obtain,

$$E'_{12} = c_2 \int_{t_1}^{t_2} v_c v(t) dt + c_3 d_{12} + c_4 \int_{t_1}^{t_2} \frac{v(t)}{v_c} dt. \quad (24)$$

To prove that $E'_{12} \leq E_{12}$, we must show that $(E_{12} - E'_{12}) \geq 0$. Using Equations 21 and 24, we can write,

$$E_{12} - E'_{12} = \int_{t_1}^{t_2} \Big[c_1 a^2(t) + c_2 v^2(t) + c_4\Big] dt + c_3 d_{12}$$
$$- c_2 \int_{t_1}^{t_2} v_c v(t) dt - c_3 d_{12} - c_4 \int_{t_1}^{t_2} \frac{v(t)}{v_c} dt$$
$$= c_1 \int_{t_1}^{t_2} a^2(t) dt$$
$$+ \frac{c_2}{v_c} \int_{t_1}^{t_2} [v_c(t) - v(t)] \left[\frac{c_4}{c_2} - v(t) v_c\right] .dt$$
$$\therefore E_{12} - E'_{12} \geq 0,$$

since $v(t) \leq v_c \leq \sqrt{\frac{c_4}{c_2}}$. For the section between t_3 and t_4, we can follow a similar argument to yield,

$$E_{34} - E'_{34} = c_1 \int_{t_3}^{t_4} a^2(t) dt$$
$$+ \frac{c_2}{v_c} \int_{t_3}^{t_4} [v_c(t) - v(t)] \left[\frac{c_4}{c_2} - v(t) v_c\right] dt.$$
$$\therefore E_{34} - E'_{34} \geq 0,$$

since $v(t) \geq v_c \geq \sqrt{\frac{c_4}{c_2}}$. In general we can replace any number of such sections crossing $\sqrt{\frac{c_4}{c_2}}$ to yield another velocity profile with lower energy covering the same distance moving at $\sqrt{\frac{c_4}{c_2}}$. Hence, once the velocity profile hits $\sqrt{\frac{c_4}{c_2}}$, there is no reason to deviate from this value except at the boundary (initial and final conditions). ■

D. Comparisons with trapezoidal velocity profile

A trapezoidal velocity profile is commonly used for its ease of implementation. A trapezoidal velocity profile (see Figure 7) consists of a constant acceleration section, followed by a constant velocity section, followed by a constant deceleration section. In [13], Wang et al. computed the optimal trapezoidal velocity profile for traveling a given distance D. However, their result is only applicable in the case when there is no bound on the maximum velocity of the robot. Hence, we can only compare their method for the case when there is no bound on the maximum velocity, and not the general solution that we present in the next section.

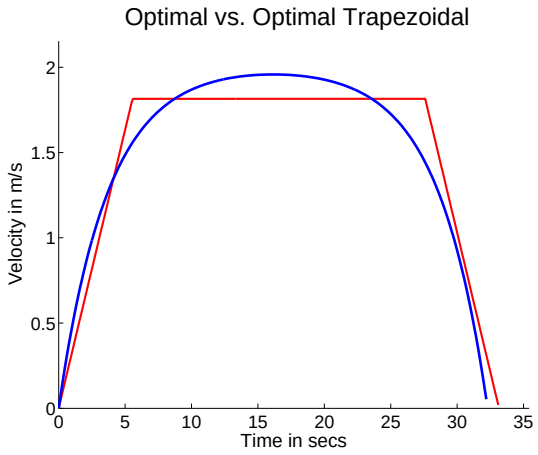

Fig. 7. Optimal trapezoidal profile computed using the same energy function shown together with the general optimal profile for traveling $D = 50m$. The general optimal profile we compute gains higher savings with respect to the trapezoidal profile while accelerating and decelerating. This yields higher energy savings when the total distance to travel is less, a scenario commonly seen when the robot has to frequently start and stop.

Figure 7 shows the optimal profile and optimal trapezoidal profile computed for traveling a distance of $D = 50m$. We can observe that the optimal trapezoidal profile closely matches with the general optimal solution except while accelerating and decelerating. The general optimal profile we compute gains higher savings with respect to the trapezoidal profile while accelerating and decelerating. Hence, the percentage energy savings for the general optimal profile are higher when the robot has to travel for shorter distances. For example, the optimal profile yields 1.94% savings when traveling $1m$, while the savings drop to 0.32 when $D = 100m$ for the parameters calculated on our custom robot. In situations where the robot has to frequently stop, following an optimal profile would result in more energy savings and consequently longer run-time. It should be noted that these figures are highly system-specific and the savings will vary from robot to robot. However, for all systems, the velocity profile computed in this work is guaranteed to minimize the energy consumption for the stated assumptions.

V. General solution incorporating maximum velocity bound

The optimal profile given in Section IV does not satisfy any bound on the maximum velocity imposed by the physical limitations of the robot. In this section, we solve for the optimal velocity profile for *Problem 2*, with a bound on the maximum velocity $v(t) \leq v_m$. We also consider the general case where the initial and the final velocities of the robot can be non-zero,

$$v(0) = v_0, \quad v(t_f) = v_f$$

subject to $v_0, v_f \leq v_m$. The non-zero initial and final velocities are useful in computing the optimal velocity profile when

the given path consists of multiple segments, with different velocity bounds for each segment. We will consider this case in Section VI. In this section, we first present the structure of optimal profile under different conditions and then present the solution for each.

A. Structure of optimal profile

If either v_0 or v_f is greater than v_m, no valid solution exists. Otherwise, depending on the value of v_m and D, the optimal velocity profile can belong to one of the following two cases.

CASE 1: Unconstrained optimal profile does not violate bound $v(t) \leq v_m$

In the case that the optimal velocity profile computed in Section IV does not exceed the bound v_m, then this profile is a valid solution for the constrained case too. This happens when $v_m \geq \sqrt{\frac{c_4}{c_2}}$. Additionally, in the case when the distance to travel D is very small, the optimal velocity profile may not have enough time to reach v_m or $\sqrt{\frac{c_4}{c_2}}$. This situation can be seen in Figure 5 when $D = 5m$.

While solving for the optimal profile in Equation 15, we considered only zero initial and final velocity boundary conditions. Here, instead we extend this result for possibly non-zero v_0 and v_f as the initial and final velocities. By following a process similar to that described in Section IV we get,

$$
\begin{aligned}
s_1 &= \frac{(v_0 - v_f)(1 - e^{-kt_f} - kt_f) + Dk(1 - e^{-kt_f})}{e^{kt_f}(2 - kt_f) + e^{-kt_f}(2 + kt_f) - 4}, \\
s_2 &= \frac{(v_0 - v_f)(1 - e^{kt_f} + kt_f) - Dk(1 - e^{kt_f})}{e^{kt_f}(2 - kt_f) + e^{-kt_f}(2 + kt_f) - 4}, \\
s_3 &= 2c_1(s_1 + s_2) - c_3 - v_0, \\
s_4 &= -\frac{s_1 - s_2}{k}.
\end{aligned} \tag{25}
$$

The resulting profiles can be obtained by substituting the above in Equations 12-14. Figure 8 shows the resulting velocity profile obtained for traveling $50m$ with $v_0 = 0.2$, $v_f = 3.8$ and $v_m = 4m/s$.

CASE 2: Unconstrained optimal profile violates the bound $v(t) \leq v_m$

If the unconstrained optimal profile violates the bound v_m, the constrained optimal velocity profile will consist of unconstrained $\mathcal{U}$ ($v(t) < v_m$) and constrained arcs $\mathcal{C}$ ($v(t) = v_m$) joined together at *corner points*. We show that there exists an optimal profile with a $\mathcal{U}-\mathcal{C}-\mathcal{U}$ sequence having *corner points* at times $t = t_1$ and $t = t_f - t_2$, along with its degenerate cases $(\mathcal{U}-\mathcal{C}, \mathcal{C}-\mathcal{U}, \mathcal{C})$ when either or both of t_1 and t_2 equal to 0.

By definition, there cannot be any $\mathcal{U}-\mathcal{U}$ or $\mathcal{C}-\mathcal{C}$ sequence, as these do not include any *corner points*. Using this and the following lemma, we show that the constrained velocity profile in this case is limited to the above given sequences.

Lemma 5.1: The optimal velocity profile cannot consist any sequence of the form $\mathcal{C} - \mathcal{U} - \mathcal{C}$.

Proof: Consider any velocity profile consisting of a $\mathcal{C} - \mathcal{U} - \mathcal{C}$ sequence covering distance D. We can replace this $\mathcal{C}-\mathcal{U}-\mathcal{C}$ sequence with a single $\mathcal{C}$ section, so that the resulting velocity profile covers the same distance and consumes energy less than the original profile.

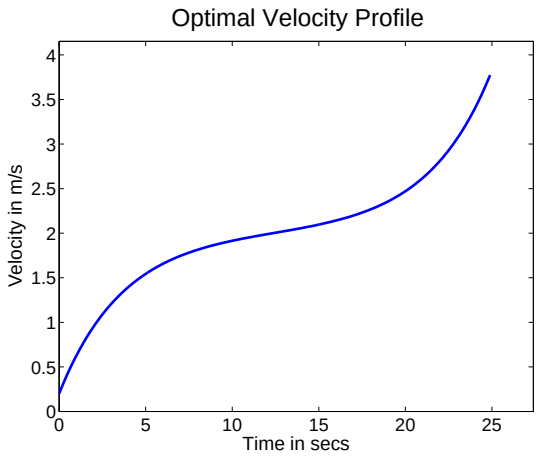

Fig. 8. Optimal velocity profile for the case when $v_m > \sqrt{\frac{c_4}{c_2}}$ consists of a single unconstrained arc. Here, $v_0 = 0.2m/s$, $v_m = 4m/s$ and $v_f = 3.8m/s$ for traveling $50m$ with $\sqrt{\frac{c_4}{c_2}} = 2m/s$.

The proof is similar to that of Lemma 4.1. Let $v(t)$ be any velocity profile that contains a $\mathcal{C} - \mathcal{U} - \mathcal{C}$ sequence. That is, $v(t) = v_m(t)$ for $t_0 \leq t \leq t_1$ and $t_2 \leq t \leq t_3$ and $v(t) < v_m$ between $t_1 \leq t \leq t_2$. The energy consumption of this profile for traveling a distance $D = d_{01} + d_{12} + d_{23}$,

$$E = E_{01} + E_{12} + E_{23},$$

where E_{ij} is the energy spent in traveling d_{ij} for $v(t)$. We construct another velocity profile that is identical to $v(t)$ in $[t_0, t_1]$ and $[t_2, t_3]$ but covers the section d_{12} at $v(t) = v_m$. The energy consumption for this new profile is given by,

$$E' = E_{01} + E'_{12} + E_{23}.$$

By following a process very similar to that in Lemma 4.1, we can show that $E'_{12} \leq E_{12}$ leading to $E' \leq E$. Hence, any $\mathcal{C}-\mathcal{U}-\mathcal{C}$ sequence can be replaced by a single $\mathcal{C}$ segment to reduce the energy consumption. Hence, the optimal velocity profile will never consist of a $\mathcal{C}-\mathcal{U}-\mathcal{C}$ sequence. ■

We now show how to obtain the solution for this case in closed form. Specifically, we show how to obtain $v(t)$ for the unconstrained and constrained arcs and compute the corner points t_1 and t_2.

B. Solution

We begin by writing the velocity constraint in the form of state inequality $\bar{S} = (v(t) - v_m) \leq 0$. The state inequality $\bar{S}$ is converted into a control equality and interior point constraint by differentiating $\bar{S}$ once leading to,

$$
\begin{aligned}
\bar{S}^{(1)} &= \dot{v}(t) = u. \\
v(t_1) &= v_m
\end{aligned} \tag{26}
$$

Along the unconstrained arc, the state transition is governed by Equation 1. On the constrained arc, the state transition is given by,

$$\dot{\mathbf{X}}(t) = \begin{bmatrix} \dot{x}(t) \\ \dot{v}(t) \end{bmatrix} = \begin{bmatrix} v_m \\ 0 \end{bmatrix} \tag{27}$$

The Hamiltonian is augmented with the control equality constraint in $[t_1, t_f - t_2]$ and is given by,

$$\begin{aligned}\hat{H} &= c_1 a^2(t) + c_2 v^2(t) + c_3 v(t) + c_4 \\ &+ \lambda_1(t) v(t) + \lambda_2(t) a(t) + \mu(t) a(t)\end{aligned} \tag{28}$$

where $\mu(t)$ is the slack variable associated with the control constraint. In the interval $[0, t_1]$ and $[t_f - t_2, t_f]$, the Hamiltonian is given by,

$$\begin{aligned}H &= c_1 a^2(t) + c_2 v^2(t) + c_3 v(t) \\ &+ c_4 + \lambda_1(t) v(t) + \lambda_2(t) a(t)\end{aligned} \tag{29}$$

The interior point constraint is given by,

$$G = \xi(v(t) - v_m) \tag{30}$$

The three necessary conditions given in Equation 11 are used to obtain the optimal profile in the time interval $[0, t_1]$ and $[t_f - t_2, t_f]$. On the constraint boundary, i.e., $t \in [t_1, t_f - t_2]$, the following necessary conditions must hold,

$$\dot{\mathbf{X}}^*(t) = \frac{\partial H}{\partial \boldsymbol{\lambda}} \quad \dot{\boldsymbol{\lambda}}^*(t) = \frac{\partial \hat{H}}{\partial \mathbf{X}} \quad 0 = \frac{\partial \hat{H}}{\partial a} \tag{31}$$

Also, on the two corners ($t = t_1$ and $t = t_f - t_2$), the following conditions must hold for the optimal solution [6],

$$\begin{aligned}H(t_1^+) &= H(t_1^-) + \left.\frac{\partial G}{\partial t}\right|_{t_1} \\ \boldsymbol{\lambda}(t_1^+) &= \boldsymbol{\lambda}(t_1^-) - \left[\frac{\partial G}{\partial \mathbf{X}}\right]^T_{t_1} \\ H((t_f - t_2)^+) &= H((t_f - t_2)^-) \\ \boldsymbol{\lambda}((t_f - t_2)^+) &= \boldsymbol{\lambda}((t_f - t_2)^-)\end{aligned} \tag{32}$$

Using the conditions given above, we can solve for the optimal control and velocity profile in terms of the constants for the off-boundary exponential curves and time t_1, t_2 and t_f. The optimal velocity profile in this case is given by,

$$v^*(t) = \begin{cases} s_1\left(e^{kt} + e^{k(2t_1 - t)} - (1 + e^{2kt_1})\right) + v_0, \\ \qquad\qquad 0 \le t \le t_1 \\ v_m, \qquad\qquad t_1 \le t \le t_f - t_2 \\ s_2\left(e^{-k(t_f - t - 2t_2)} + e^{k(t_f - t)} - (1 + e^{2kt_2})\right) + v_f, \\ \qquad\qquad t_f - t_2 \le t \le t_f. \end{cases} \tag{33}$$

We can obtain the values of these constants and times using the initial and final conditions, the transversality condition given in Equation 17 and the interior point constraint $v^*(t) = v_m, \quad t_1 \le t \le t_f - t_2$ as,

$$\begin{aligned}s_1 &= -\frac{(v_m - v_0)}{(e^{kt_1} - 1)^2}, \\ s_2 &= -\frac{v_m - v_f}{(e^{kt_2} - 1)^2}, \\ t_1 &= \frac{1}{k}\ln\Big(\frac{c_4 + c_2 v_m^2 - 2c_2 v_0 v_m}{c_4 - c_2 v_m^2} \\ &\quad + \frac{2(c_2 v_m (c_4 - c_2 v_0 v_m)(v_m - v_0))^{\frac{1}{2}}}{c_4 - c_2 v_m^2}\Big), \\ t_2 &= \frac{1}{k}\ln\Big(\frac{c_4 + c_2 v_m^2 - c_2 v_f v_m}{c_4 - c_2 v_m^2} \\ &\quad + \frac{2(c_2 v_m (c_4 - c_2 v_f v_m)(v_m - v_f))^{\frac{1}{2}}}{c_4 - c_2 v_m^2}\Big).\end{aligned} \tag{34}$$

and the final time can then be calculated by using the total distance to travel and the distances traveled in the two exponential curves.

$$t_f = t_1 + t_2 + \frac{x^*(t_f - t_2) - x^*(t_1)}{v_m}.$$

It is easy to see that if v_0 or v_f is equal to v_m, then $t_1 = 0$ or $t_2 = 0$ respectively.

C. Examples and observations

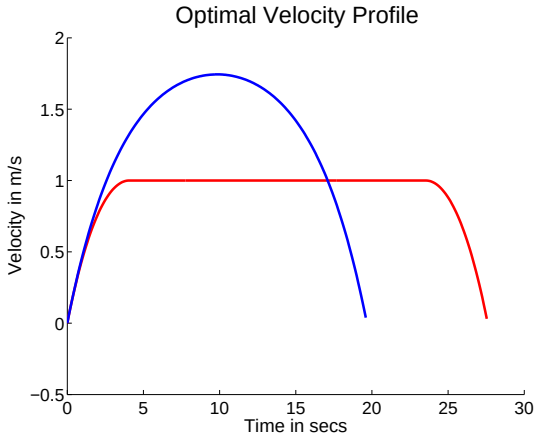

Fig. 9. Optimal Velocity ($v^*(t)$) profile obtained for maximum velocity bound $v_m = 1m/s$. The constrained velocity profile consists of exponential acceleration and deceleration curves with the constraint boundary in the middle. This profile is not the same as that obtained from unconstrained solution by setting velocity to v_m wherever it exceeds.

Figure 9 shows the optimal velocity profile obtained for traveling a distance of $25m$ with the maximum velocity bound set to $v_m = 1m/s$ and $v_0, v_f = 0$. It can be observed that the optimal velocity profile follows an exponential curve till it hits the boundary at $t_1 = 4.06s$ and then stays on the constraint boundary, before following a symmetric exponential curve to zero. The corresponding optimal velocity profile obtained without any bounds (Section IV) is shown along with the unconstrained solution. The time taken by the constrained solution is higher than that of the unconstrained solution. The corresponding optimal control is shown in Figure 10.

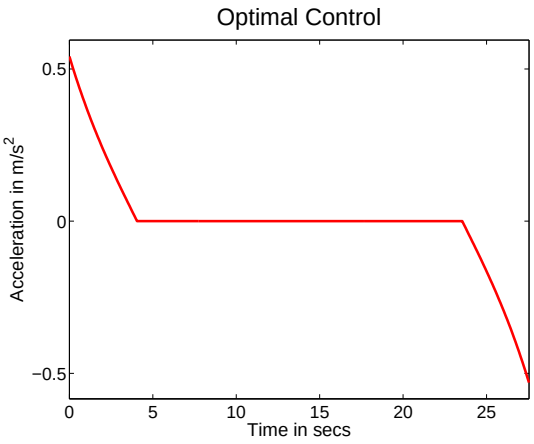

Fig. 10. Optimal control for the case with bound on maximum velocity. Note that the control is zero whenever the velocity is on the constraint boundary (see Figure 9).

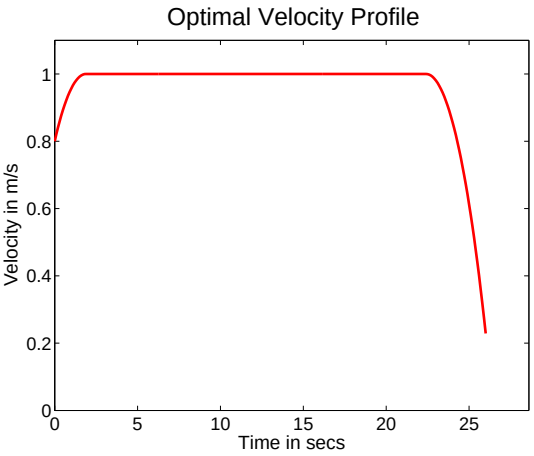

Fig. 11. Optimal velocity profile with $v_0 = 0.3m/s$, $v_m = 0.4m/s$ and $v_f = 0.1m/s$ for traveling $30m$.

Figure 11 shows the optimal velocity profile obtained for the traveling a distance of $30m$, with velocity bound $v_m = 0.4m/s$ and initial and final velocities $v_0 = 0.3m/s$ and $v_f = 0.1m/s$ respectively. Note that the acceleration and deceleration times are different in this case.

The following theorem summarizes the results for all the cases considered.

Theorem 5.2: The optimal velocity profile that minimizes the energy consumption given by Equation 6 to travel a specified distance D is given by,

- Equations 16 and 15 when there is no bound on the maximum velocity of the robot and initial and final velocities are both zero,
- Equations 16 and 25 when the maximum velocity bound $v_m > \sqrt{\frac{c_4}{c_2}}$ and initial and final velocities can be non-zero,
- Equations 33 and 34 when the maximum velocity bound $v_m \leq \sqrt{\frac{c_4}{c_2}}$ and initial and final velocities can be non-zero.

The final time t_f in each case can be obtained by from Equation 17.

VI. Optimal Profile over Multiple Segments

We now use the general optimal velocity profile solution given above to solve for the problem of finding the optimal velocity profile over a path consisting of N segments (see Figure 12). Depending on the surface on which a car-like robot operates, the maximum feasible speed without either slipping or overturning for each segment will depend on the radius of the segment. Hence, for each segment, we have the maximum allowable velocity for the robot $v_m(i)$ and the distance to travel $D(i)$, $1 \leq i \leq N$.

The robot initially starts at and returns to rest, i.e., $v_0(1) = 0$ and $v_f(N) = 0$. The velocities $v_0(i)$ and $v_f(i)$ can be non-zero for all other intermediate segments. We can compute the optimal velocity profile for a given segment, if we know the $v_0(i)$ and $v_f(i)$ that the optimal velocity profile uses.

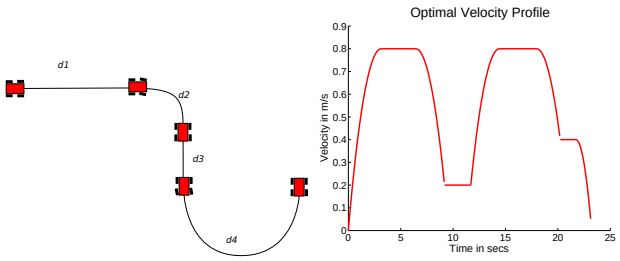

Fig. 12. **Left:** Typical path for a robot composed of two straight line segments and two turns of different radii. Segments have different maximum allowable velocities, depending on their radii. **Right:** Optimal velocity profile with different bounds for different segments. The given path consists of 4 segments with bounds $v_m = \{0.8, 0.2, 0.8, 0.4\}m/s$ and distances $D = \{6, 0.5, 6, 1\}m$

A. Greedy Strategy

From Lemmas 4.1 and 5.1, we proved that the optimal profile travels at $\min\{v_m, \sqrt{\frac{c_4}{c_2}}\}$ except at the boundaries. This suggests that the optimal profile over multiple segments will try to remain as close to $\min\{v_m(i), \sqrt{\frac{c_4}{c_2}}\}$ as possible. We can thus come up with a greedy strategy where we pick $v_0(i) = \min\{v_m(i-1), v_m(i)\}$ and $v_f(i) = \min\{v_m(i), v_m(i+1)\}$ as the boundary values for segment i. That is, for each segment boundary, we choose the highest feasible value as the initial and final velocity.

We can prove that if the distances $D(i)$ are *sufficiently large*, the greedy strategy is optimal. We first define what it means for $D(i)$ to be sufficiently large.

Sufficiently Large Distances $D^*(v_m(i))$: Given a velocity bound v_m, any distance to travel for a segment D is said to be *sufficiently large*, if the optimal velocity profile $v^*(t)$, with $v_0 = 0$ and $v_f = 0$ has at least one point where $v^*(t) = v_m$, i.e., the optimal profile contains a constrained arc $\mathcal{C}$.

In Equation 33, when $t_1 = t_f - t_2$ the optimal velocity profile contains exactly one point $t = t_1$ where $v^*(t) = v_m$.

By substituting $t_1 = t_f - t_2$ and $v_0 = v_f = 0$ in Equation 34 we get,

$$t_1 = \frac{1}{k} \log \frac{\sqrt{\frac{c_4}{c_2}} + v_m}{\sqrt{\frac{c_4}{c_2}} - v_m}.$$

The total distance traveled in this case is given by,

$$D^*(v_m) = \frac{2v_m}{(e^{kt_1} - 1)^2} \left[(1 + e^{2kt_1})t_1 - \frac{(e^{2kt_1} - 1)}{k} \right].$$

Now if $D(i) \geq D^*(v_m(i))$, the optimal velocity profile has sufficient distance to accelerate from rest, reach v_m and return to rest. Consequently, for any $v_0, v_f \geq 0$, the optimal velocity profile has sufficient distance to reach v_m. We can show that at the boundary between two segments with *sufficiently large* distances, the optimal velocity profile will never decelerate further than $\min\{v_m(i-1), v_m(i)\}$. This proof can be constructed similar to that of Lemma 4.1, by proving that any profile decelerating below $\min\{v_m(i-1), v_m(i)\}$ can be replaced by another profile decelerating only up to $\min\{v_m(i-1), v_m(i)\}$ and the energy consumption strictly increases. Hence, the greedy strategy yields the optimal when all $D(i) \geq D^*(v_m(i))$

Lemma 6.1: Consider a segment boundary i such that the distances $D(i) \geq D^*(i)$ and $D(i+1) \geq D^*(i+1)$. Then there exists an optimal velocity profile which leaves the i^{th} segment and enters the $(i+1)^{th}$ with velocity $v_f(i) = v_0(i+1) = \min\{v_m(i), v_m(i+1)\}$.

Proof: The key observation from the solution presented in Section V is that the optimal velocity profile starting at any initial velocity always accelerates toward v_m and stays there except at the boundary. Hence, using a procedure similar to that in Lemma 4.1 we can show that at any segment boundary, if a velocity profile decelerates further than $\min\{v_m(i), v_m(i+1)\}$, it consumes more energy than another profile that only decelerates up to $\min\{v_m(i), v_m(i+1)\}$.

Consider the i^{th} boundary such that $v_m(i) > v_m(i+1)$. Consider a velocity profile $v(t)$ that crosses the segment boundary at a velocity $v < v_m(i+1)$. As distance $D(i+1) \geq D^*(i+1)$, from the solution presented in Section V, we know that the optimal profile in the $(i+1)^{th}$ segment will accelerate up to $v_m(i+1)$ and stay there. Now, consider another velocity profile $v'(t)$ which crosses the segment boundary at $v' = v_m(i+1)$. Again from Section V, the optimal velocity profile will remain at $v_m(i+1)$ till the next segment boundary. Note the first profile $v(t)$ will constain a section where it decelerates to a velocity below $v_m(i+1)$ and then again accelerates back to $v_m(i+1)$.

Using a proof similar to that in Lemma 5.1, we can show that the energy consumption for $v'(t)$ is less than that for $v(t)$ for this section. Hence, the optimal velocity profile will not decelerate further than $\min\{v_m(i), v_m(i+1)\}$ at the segment boundaries. As a result, the greedy yields optimal solution in the case where all distances $D(i) \geq D^*(i)$. ■

When the distances $D(i) < D^*(v_m(i))$, the greedy strategy does not yeild an optimal solution. Consider a segment boundary such that $D(i) \ll D^*(v_m(i))$. The greedy strategy forces the velocity profile to achieve $v_f(i) = v_m(i)$ leading to higher energy consumption. The optimal on the other hand will reach a much lower value for $v_f(i)$. For such cases, we can discretize the velocity at the segment boundary and use dynamic programming to yeild the solution.

B. Dynamic Programming

Let V_{max} be the maximum of $\{v_m(i), \forall i\}$ over all segments. We then discretize the velocity space at the segment boundary into M equal partitions $v^{(k)} = \frac{k}{M} V_{max}, 0 \leq k \leq M$. Let $C(v^{(k)}, i)$ be the cost to reach the velocity $v^{(k)}$ at the i^{th} segment boundary. Let $E(v_0, v_m, v_f)$ be a function which gives the energy consumption for an optimal velocity profile in a segment starting with v_0 and ending with v_f, using the solution in Theorem 5.2. If either $v_0 > v_m$ or $v_f > v_m$ then the function returns the cost as $E(v_0, v_m, v_f) = \infty$.

We can then use the following recurrence for the i^{th} segment boundary:

$$C(v^{(k)}, i) = \min_{0 \leq j \leq M} \left(C(v^{(j)}, i-1) + E(v^{(j)}, v_m(i), v^{(k)}) \right), \quad 1 \leq k \leq M.$$

Since the robot initially starts from rest, we have the following,

$$C(v^{(k)}, 0) = \begin{cases} 0 & k = 0, \\ \infty & 1 \leq k \leq M. \end{cases}$$

The solution can be obtained by backtracking from $C(v^{(0)}, N)$ and finding optimal segment boundary velocity values. The optimal velocity profile can then be constructed using these optimal boundary velocity values to find individual segment profiles using Theorem 5.2.

Figure 12 (right) shows the optimal velocity profile obtained using above dynamic programming for a path consisting of 4 segments. The velocity bounds for these segments are $v_m = \{0.8, 0.2, 0.8, 0.4\} m/s$. This solution is optimal up to numerical precision along the segment boundaries only and exact everywhere else.

VII. Experiments

To test the validity of our results, we performed experiments using our custom robot. We used the energy measurement circuit (described in Section III) to compute the energy consumption for motion of the robot moving along a straight line. We begin by describing the experimental setup and then present the results of these experiments.

The experiments were performed on the smooth corridor surface. As described in Section III, the robot was first calibrated to obtain the model parameters for both the surfaces (given in Table I). Using Theorem 5.2, the optimal profile is computed for the given distance. We then sample this profile every $100ms$ and store it in a table on the microcontroller.

We compare the energy consumption of the optimal profile with two commonly-used trapezoidal profiles. The maximum speeds for these profiles are chosen as $1m/s$ and $2m/s$, so that the robot covers the same distance taking more and less time than the optimal respectively. We perform these comparisons for two distances $D = 20, 45m$.

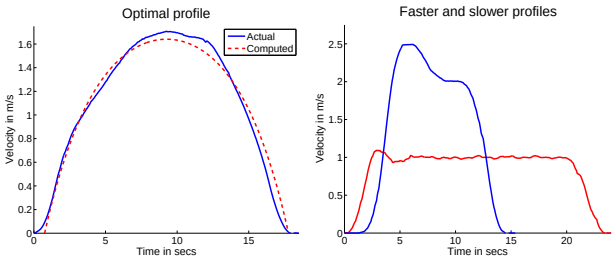

Fig. 13. **Left:** Optimal velocity profile executed by the robot for traveling $20m$ in $18.4s$ while consuming $296J$ energy. The optimal profile computed using Theorem 5.2 is shown as dashed. **Right:** Sub-optimal velocity profiles executed by the robot for traveling $20m$ at maximum set velocities of $1m/s$ and $2m/s$. The energy consumption for these profiles is $303J$ and $319J$.

Figure 13 shows the optimal, slower and faster velocity profiles executed by the robot in the corridor. The optimal profile computed is also shown in Figure 13 as dashed. As can be seen, the actual profile executed by the robot follows closely the desired profiles, albeit with small deviations arising due to noise in encoders and disturbances on the surface. The energy consumption in the robot for the optimal profile was $296J$ as against $303J$ and $319J$ for the slower and faster profiles.

We repeated these trials for a longer distance of $45m$. Table II shows the comparison of the energy consumption for all the trials conducted. As can be observed, the optimal profile consumes lesser energy than the two sub-optimal profiles.

TABLE II
ENERGY CONSUMPTION DURING EXPERIMENTS

D (m)	$E_{opt}(J)$	$E_{slow}(J)$	$E_{fast}(J)$
20	296	303	319
45	656	694	696

VIII. CONCLUSION

In this work, we studied the problem of computing a velocity profile for a car-like robot so as to minimize the energy consumed while traveling along a given path on a flat surface. We presented closed form solutions for two cases: no constraints on the robot's speed, and a single upper-bound on the speed. We also studied a general case where the robot's path is composed of segments and we are given a speed upper-bound for each segment. For example, the robot's path can be composed of circular and straight-line segments. When the robot is following the circular sub-path, the maximum speed it can achieve can be less than the maximum speed for the straight component. These bounds may vary depending on the surface properties. For this general case, we presented a dynamic programming solution which builds on the solution for the single-bound case.

In addition, we presented a calibration procedure for obtaining robot's internal parameters related to energy consumption. We demonstrated the utility of the calibration procedure and the algorithms presented in the paper with experiments performed on a custom-built robot.

Throughout the paper, we assumed that the robot's path is given. Our next step is to study the problem of computing the optimal path that minimizes the energy consumption. From our initial investigation, it does not seem like minimum energy paths exhibit the same structure as the shortest-path (Dubins') curves.

ACKNOWLEDGMENT

This work is supported by NSF projects 0916209, 0917676 and 0936710.

REFERENCES

[1] *DC Motors, Speed Controls, Servo Systems: An Engineering Handbook*. Electro-Craft Corporation, 1977.
[2] D. Balkcom and M. Mason. Time optimal trajectories for bounded velocity differential drive vehicles. *The International Journal of Robotics Research*, 21(3):199, 2002.
[3] H. Chitsaz, S. LaValle, D. Balkcom, and M. Mason. Minimum wheel-rotation paths for differential-drive mobile robots. *The International Journal of Robotics Research*, 28(1):66, 2009.
[4] B. Donald, P. Xavier, J. Canny, and J. Reif. Kinodynamic motion planning. *J. ACM*, 40(5):1048–1066, 1993.
[5] L. Dubins. On curves of minimal length with a constraint on average curvature, and with prescribed initial and terminal positions and tangents. *American Journal of Mathematics*, 79(3):497–516, 1957.
[6] D. Hull. *Optimal control theory for applications*. Springer Verlag, 2003.
[7] C. Kim and B. Kim. Minimum-Energy Rotational Trajectory Planning for Differential-Driven Wheeled Mobile Robots. In *Proc. 13th Int. Conf. on Advanced Robotics*, pages 265–270, 2007.
[8] C. Kim and B. Kim. Minimum-energy translational trajectory generation for differential-driven wheeled mobile robots. *Journal of Intelligent and Robotic Systems*, 49(4):367–383, 2007.
[9] D. Kirk. *Optimal Control Theory: An Introduction*. Prentice Hall, 1970.
[10] Y. Mei, Y. Lu, Y. Hu, and C. Lee. Energy-efficient motion planning for mobile robots. In *IEEE International Conference on Robotics and Automation*, volume 5, 2004.
[11] J. Reeds and L. Shepp. Optimal Paths for A Car That Goes Both Forwards and Backwards. *Pacific Journal of Mathematics*, 145(2):367–393, 1990.
[12] Z. Sun and J. Reif. On finding energy-minimizing paths on terrains. *IEEE Transactions on Robotics*, 21(1):102–114, 2005.
[13] G. Wang, M. Irwin, P. Berman, H. Fu, and T. La Porta. Optimizing sensor movement planning for energy efficiency. In *Proceedings of the 2005 international symposium on Low power electronics and design*, page 220. ACM, 2005.

APPENDIX A
PROOF: UNCONSTRAINED SOLUTION

The state transition equation can be written as,

$$\dot{\mathbf{X}}(t) = \begin{bmatrix} \dot{x}(t) \\ \dot{v}(t) \end{bmatrix} = \begin{bmatrix} v(t) \\ a(t) \end{bmatrix} \tag{35}$$

The objective is to find a velocity profile $v^*(t)$ which minimizes the total energy required for motion given by the following cost functional,

$$J = \int_0^{t_f} \Big[c_1 a^2(t) + c_2 v^2(t) + c_3 v(t) + c_4 \Big] dt, \tag{36}$$

where the final time t_f is kept a free variable. The initial boundary conditions are given as,

$$x(0) = 0, \quad v(0) = 0, \tag{37}$$

and the final boundary conditions are given as,

$$x(t_f) = D, \quad v(t_f) = 0. \tag{38}$$

Hamiltonian: The hamiltonian $H(\mathbf{X}, \boldsymbol{\lambda}, u, t)$ is defined as,

$$H(\mathbf{X}, \boldsymbol{\lambda}, u, t) = J + \lambda_1(t)\dot{x}(t) + \lambda_2(t)\dot{v(t)}, \tag{39}$$

where $\lambda_1(t)$ and $\lambda_2(t)$ are the Lagrange multipliers, also called the co-state variables which include the state transition equations as a constraint to the objective.

When there is no bound on the maximum velocity, the Hamiltonian for this problem can be obtained using Equations 35 and 36 as,

$$\begin{aligned} H(\mathbf{X}(t), a(t), \boldsymbol{\lambda}(t), t) \quad &= c_1 a^2(t) + c_2 v^2(t) + c_3 v(t) \\ &+ c_4 + \lambda_1(t)v(t) + \lambda_2(t)a(t) \end{aligned} \tag{40}$$

where the acceleration $a(t)$ is the control.

The three necessary conditions for $a^*(t)$ to optimize the Hamiltonian [9] for all time $t \in [0, t_f]$ are given as,

$$\dot{\mathbf{X}}^*(t) = \frac{\partial H}{\partial \boldsymbol{\lambda}}, \quad \dot{\boldsymbol{\lambda}}^*(t) = -\frac{\partial H}{\partial \mathbf{X}}, \quad 0 = \frac{\partial H}{\partial a} \tag{41}$$

By substituting we get,

$$\begin{aligned} \dot{x}(t) &= v(t), \\ \dot{v}(t) &= a(t), \\ \dot{\lambda_1}(t) &= 0, \\ \dot{\lambda_2}(t) &= 2c_2 v(t) + c_3 + \lambda_1, \\ \lambda_2(t) &= -2c_1 a(t), \\ \therefore \lambda_2(t) &= -2c_1 \dot{v}(t). \end{aligned}$$

Using the last two equations, we can write,

$$\begin{aligned} -2c_1\ddot{v}(t) &= 2c_2 v(t) + c_3 + \lambda_1, \\ 2c_1\ddot{v}(t) + 2c_2 v(t) + c_3 + \lambda_1 &= 0. \end{aligned}$$

We can solve for this second order differential equation to yield,

$$v^*(t) = s_1 e^{kt} + s_2 e^{-kt} - \left(\frac{c_3 + s_3}{2c_1}\right) \tag{42}$$

where $k = \sqrt{\frac{c_2}{c_1}}$ and $s_1 - s_4$ are constants and $\lambda_1 = s_3$.

Applying the state transition equations, we can get the optimal control and states given as,

$$a^*(t) = k s_1 e^{kt} - k s_2 e^{-kt} \tag{43}$$

$$x^*(t) = \frac{s_1 e^{kt}}{k} - \frac{s_2 e^{-kt}}{k} - \left(\frac{c_3 + s_3}{2c_1}\right) t + s_4. \tag{44}$$

We can solve for $s_1 - s_4$ in terms of the final time t_f by substituting the boundary conditions given in Equations 37 and 38 for $v^*(t)$ and $x^*(t)$. We obtain,

$$\begin{aligned} s_1 &= -\frac{Dk}{kt_f + e^{kt_f}(kt_f - 2) + 2}, \\ s_2 &= s_1 e^{kt_f}, \\ s_3 &= 2c_1(s_1 + s_2) - c_3, \\ s_4 &= -\frac{s_1 - s_2}{k}. \end{aligned} \tag{45}$$

By substituting in Equations 43-44 we obtain,

$$\begin{aligned} a^*(t) &= D\left(\frac{c_2}{c_1}\right)\left(\frac{e^(kt_f - t) - e^(kt)}{kt_f + e^{kt_f}(kt_f - 2) + 2}\right), \\ v^*(t) &= D\sqrt{\frac{c_2}{c_1}}\left(\frac{(1 + e^{kt_f} - (e^{k(t_f - t)} + e^{kt}))}{kt_f + e^{kt_f}(kt_f - 2) + 2}\right), \\ x^*(t) &= D\left(\frac{(e^{k(t_f - t)} - e^{kt}) - (e^{kt_f} - 1) + kt(e^{kt_f} + 1)}{kt_f + e^{kt_f}(kt_f - 2) + 2}\right). \end{aligned} \tag{46}$$

Since the final time is free, it can be solved for using the additional boundary condition (known as the transversality condition) given by,

$$H(\mathbf{X}^*(t_f), a^*(t_f), \boldsymbol{\lambda}^*(t_f), t_f) = 0. \tag{47}$$

Substituting Equations 43-44 and 45 above results in,

$$(D\frac{c_2}{c_1} + 2)(1 - e^{kt_f}) + \sqrt{\frac{c_4}{c_1}} kt_f (1 + e^{kt_f}) = 0, \tag{48}$$

which is an equation in single variable t_f and can be solved using existing solvers. (We used MATLAB's `solve` function). Alternatively, if the final time is fixed, we can directly substitute this given value in Equation 46 to find $v^*(t)$.

Appendix B
Proof: Constrained Solution

We begin by writing the velocity constraint in the form of state inequality $\bar{S} = (v(t) - v_m) \leq 0$. The state inequality $\bar{S}$ is converted into a control equality and interior point constraint by differentiating $\bar{S}$ once leading to,

$$\begin{aligned} \bar{S}^{(1)} &= \dot{v}(t) = u. \\ v(t_1) &= v_m \end{aligned} \tag{49}$$

Along the unconstrained arc, the state transition is governed by Equation 35. On the constrained arc, the state transition is given by,

$$\dot{\mathbf{X}}(t) = \begin{bmatrix} \dot{x}(t) \\ \dot{v}(t) \end{bmatrix} = \begin{bmatrix} v_m \\ 0 \end{bmatrix} \tag{50}$$

The Hamiltonian is augmented with the control equality constraint in $[t_1, t_f - t_2]$ and is given by,

$$\begin{aligned} \hat{H} &= c_1 a^2(t) + c_2 v^2(t) + c_3 v(t) + c_4 \\ &+ \lambda_1(t)v(t) + \lambda_2(t)a(t) + \mu(t)a(t) \end{aligned} \tag{51}$$

where μ is the slack variable associated with the control constraint. In the interval $[0, t_1]$ and $[t_f - t_2, t_f]$, the Hamiltonian is given by,

$$\begin{aligned} H &= c_1 a^2(t) + c_2 v^2(t) + c_3 v(t) \\ &+ c_4 + \lambda_1(t)v(t) + \lambda_2(t)a(t) \end{aligned} \tag{52}$$

The interior point constraint is given by,

$$G = \xi(t)(v(t) - v_m). \tag{53}$$

A. $0 \le t \le t_1$

Using the necessary condition $\dot{\lambda} = -\dfrac{\partial H}{\partial x}$ we get,

$$\begin{aligned} \dot{\lambda_1} &= 0, \\ \therefore \quad \lambda_1 &= s_3. \end{aligned}$$

and,

$$\dot{\lambda_2} = -\frac{\partial H}{\partial x}, \tag{54}$$

$$\therefore \quad \dot{\lambda_2} = -\left[2c_2 v(t) + c_3 + s_3\right]. \tag{55}$$

Applying the third necessary condition, $0 = \dfrac{\partial H}{\partial a}$ we get,

$$\begin{aligned} 0 &= 2c_1 a(t) + \lambda_2(t), \\ \therefore \quad \lambda_2(t) &= -2c_1 a(t). \end{aligned}$$

Differentiating the above equation we get,

$$\dot{\lambda_2(t)} = -2c_1 \ddot{v}(t).$$

From Equation 55 we can write,

$$\begin{aligned} 2c_1 \ddot{v(t)} &= 2c_2 v(t) + c_3 + s_3, \\ \therefore \quad \ddot{v}(t) - \frac{c_2}{c_1} v(t) - \frac{c_3 + s_3}{2c_1} &= 0. \end{aligned}$$

The solution for the above differential equation is given as,

$$\begin{aligned} v^*(t) &= s_1 e^{kt} + s_2 e^{-kt} - \frac{c_3 + s_3}{2c_1}, \\ a^*(t) &= s_1 k e^{kt} - s_2 k e^{-kt}, \\ x^*(t) &= \frac{s_1}{k} e^{kt} - \frac{s_2}{k} e^{-kt} - \frac{c_3 + s_3}{2c_1} t + s_4, \\ \lambda_1^*(t) &= s_3, \\ \lambda_2^*(t) &= -2c_1 a^*(t). \end{aligned}$$

Using initial conditions $x(0) = 0$ and $v(0) = v_0$, we get,

$$\begin{aligned} s_4 &= -\frac{s_1 - s_2}{k}, \\ \frac{c_3 + s_3}{2c_1} &= s_1 + s_2 - v_0. \end{aligned}$$

Putting these together we get,

$$\begin{aligned} v^*(t) &= s_1 e^{kt} + s_2 e^{-kt} - (s_1 + s_2 - v_0), \\ a^*(t) &= s_1 k e^{kt} - s_2 k e^{-kt}, \\ x^*(t) &= \frac{s_1}{k} e^{kt} - \frac{s_2}{k} e^{-kt} - (s_1 + s_2 - v_0) t - \frac{s_1 - s_2}{k}, \\ \lambda_1^*(t) &= 2c_1 s_1 + s_2 - v_0 - c_3, \\ \lambda_2^*(t) &= -2c_1 a^*(t), \end{aligned}$$

where s_1 and s_2 are two constants left to be evaluated.

B. $t_f - t_2 \le t \le t_f$

In this section, the system is governed by the same state equation as in the interval $0 \le t \le t_1$. Hence, we get a similar form for the optimal state and control given by,

$$\begin{aligned} v^*(t) &= s_1' e^{-kt_f} e^{kt} + s_2' e^{kt_f} e^{-kt} - \frac{c_3 + s_3'}{2c_1}, \\ a^*(t) &= s_1' k e^{-kt_f} e^{kt} - s_2' k e^{kt_f} e^{-kt}, \\ x^*(t) &= \frac{s_1'}{k} e^{-kt_f} e^{kt} - \frac{s_2'}{k} e^{kt_f} e^{-kt} - \frac{c_3 + s_3'}{2c_1} t + s_4', \\ \lambda_1^*(t) &= s_3', \\ \lambda_2^*(t) &= -2c_1 a^*(t). \end{aligned}$$

where $s_1' \ldots s_4'$ are the new constants to be solved for. Using the final condition, $x(t_f) = D$, we get

$$\begin{aligned} D &= \frac{s_1'}{k} - \frac{s_2'}{k} - \frac{c_3 + s_3'}{2c_1} t_f + s_4', \\ \therefore \quad s_4' &= D - \left[\frac{s_1'}{k} - \frac{s_2'}{k} - \frac{c_3 + s_3'}{2c_1} t_f\right]. \end{aligned}$$

Using the second final condition, $v(t_f) = v_f$ we get,

$$\begin{aligned} v_f &= s_1' + s_2' - \frac{c_3 + s_3'}{2c_1}, \\ \therefore \quad s_3' &= 2c_1(s_1' + s_2' - v_f) - c_3. \end{aligned}$$

The equations can then be written as,

$$\begin{aligned} v^*(t) &= s_1' e^{-k(t_f - t)} + s_2' e^{k(t_f - t)} - (s_1' + s_2' - v_f), \\ a^*(t) &= s_1' k e^{-k(t_f - t)} - s_2' k e^{k(t_f - t)}, \\ \lambda_1^*(t) &= 2c_1(s_1' + s_2' - v_f) - c_3, \\ \lambda_2^*(t) &= -2c_1 a^*(t). \end{aligned}$$

C. Corner conditions

We can now use the corner conditions to determine the unknown constants s_1, s_2, s_1', s_2'. The corner conditions state that $\lambda((t_f - t_2)^+) = \lambda((t_f - t_2)^-)$ and $v((t_f - t_2)^+) = v((t_f - t_2)^-)$ and $\mu((t_f - t_2)^+) = 0$,

$$\begin{aligned} H(t_2^+) &= H(t_2^-), \\ \therefore \quad a(t_f - t_2) &= 0, \\ \therefore \quad s_2' &= s_1' e^{-2kt_2}. \end{aligned}$$

Using the other corner condition $v((t_f - t_2)^+) = v((t_f - t_2)^-)$ we have,

$$\begin{aligned} v(t_f - t_2) &= v_m, \\ \therefore \quad s_1' e^{-kt_2} + s_1' e^{-kt_2} - (s_1' + s_1' e^{-2kt_2} - v_f) &= v_m, \\ \therefore \quad s_1' &= -\frac{v_m - v_f}{(e^{-kt_2} - 1)^2}. \end{aligned}$$

Using similar arguments at the other corner $t = t_1$ we get the final form for the optimal velocity profile as,

$$v^*(t) = \begin{cases} s_1\left(e^{kt} + e^{k(2t_1-t)} - (1+e^{2kt_1})\right) + v_0, \\ \qquad\qquad\qquad\qquad\qquad\qquad 0 \le t \le t_1 \\ v_m, \qquad\qquad\qquad\qquad\qquad t_1 \le t \le t_f - t_2 \\ s_2\left(e^{-k(t_f-t-2t_2)} + e^{k(t_f-t)} - (1+e^{2kt_2})\right) + v_f, \\ \qquad\qquad\qquad\qquad\qquad\qquad t_f - t_2 \le t \le t_f. \end{cases}$$

where,

$$s_1 = -\frac{(v_m - v_0)}{(e^{kt_1}-1)^2},$$
$$s_2 = -\frac{v_m - v_f}{(e^{kt_2}-1)^2},$$

Using the transversality condition $H(t_f) = 0$, we can determine the times t_1 and t_2 as,

$$\begin{aligned} t_1 &= \frac{1}{k}\ln\left(\frac{c_4 + c_2v_m^2 - 2c_2v_0v_m}{c_4 - c_2v_m^2} + \right. \\ &\qquad \left. \frac{2(c_2v_m(c_4 - c_2v_0v_m)(v_m - v_0))^{\frac{1}{2}}}{c_4 - c_2v_m^2}\right), \\ t_2 &= \frac{1}{k}\ln\left(\frac{c_4 + c_2v_m^2 - ca_2v_fv_m}{c_4 - c_2v_m^2} + \right. \\ &\qquad \left. \frac{2(c_2v_m(c_4 - c_2v_fv_m)(v_m - v_f))^{\frac{1}{2}}}{c_4 - c_2v_m^2}\right). \end{aligned} \tag{56}$$

and the final time can then be calculated by using the total distance to travel and the distances traveled in the two exponential curves. It is easy to see that if v_0 or v_f is equal to v_m, then $t_1 = 0$ or $t_2 = 0$ respectively.